Topic	Measuring rotational ground motions in seismological practice
Authors	**William. H. K. Lee[1)], John R. Evans[1)], Bor-Shouh Huang[2)], Charles R. Hutt[3)], Chin-Jen Lin[2)], Chun-Chi Liu[2)], and Robert L. Nigbor[4)]** [1)] U. S. Geological Survey, MS 977, 345 Middlefield Road, Menlo Park, CA 94025, USA; contact via E-mail: lee@usgs.gov; [2)] Institute of Earth Sciences, Academia Sinica, P.O. Box 1-55, Nankang, 11529 Taipei, Taiwan; [3)] U. S. Geological Survey, P.O. Box 82010, Albuquerque, NM 87198, USA; [4)] Department of Civil Engineering, University of California at Los Angeles, Los Angeles, CA 90095, USA.
Version	February 2011; **DOI: 10.2312/GFZ.NMSOP-2_IS_5.3**

Hypertext links and other references to products are provided for information only and do not constitute endorsement or warranty, expressed or implied, as to their suitability, content , usefulness, functioning, completeness, or accuracy by the United States Geological Survey.

1 Introduction

Rotational seismology is an emerging study of all aspects of rotational motions induced by earthquakes, explosions, and ambient vibrations. The subject is of interest to several disciplines, including seismology, earthquake engineering, geodesy, and earth-based detection of Einstein's gravitation waves. In this chapter, we will present basic elements of measuring rotational ground motions in seismological practice and an overview of recent observations. Because there are terms in this Chapter that may not be familiar to the readers, readers may consult either the amended **Glossary** of this manual, or for an even more detailed glossary on rotational seismology Lee (2009).

Likely rotational effects of earthquake waves together with rotations caused by soil-structure interaction have been observed for centuries (e.g., rotated chimneys, monuments, and tombstones relative to their supports). A summary of historical examples of observations on earthquake rotational effects is provided by Kozák (2009), including reproduction of the relevant sections from Mallet (1862) and Reid (1910). Figure 1 shows the rotation of the monument to George Inglis (erected in 1850 at Chatak, India) as observed by Oldham (1899) after the 1897 Great Shillong earthquake.

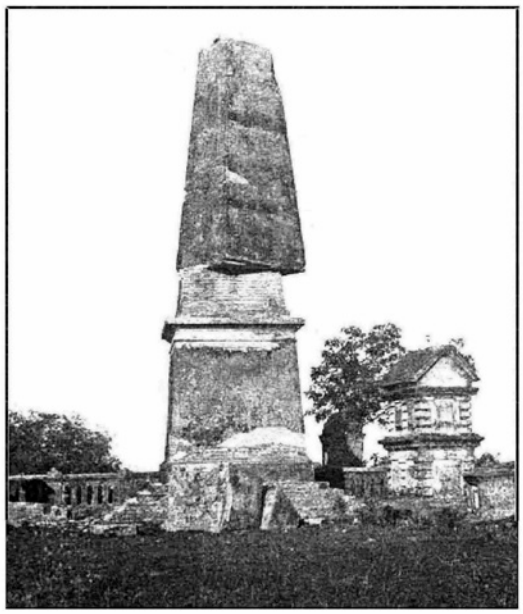

Figure 1 Rotation of the monument to George Inglis (erected in 1850 at Chatak, India) as observed by Oldham (1899) after the 1897 Great Shillong earthquake. This monument had the form of an obelisk rising about 20 m high from a base 4 m on each side. During the earthquake, the topmost 2 m section was broken off and fell to the south and the next 3 m section was thrown to the east. The remnant is about 6.5 m in height and is rotated about 15° relative to the base. Such rotations can be due to strictly translational accelerations and don't necessarily require rotational ground motion (see text).

A few early authors proposed rotational waves or at least some "vortical" motions. Many different terms were used for the rotational motion components at this early development stage. For example, "rocking" is rotation around a horizontal axis, sometimes also referred to as "tilt". Mallet (1862) proposed that rotations of a body on the Earth's surface are due to a sequence of different seismic phases emerging at different angles. Computational modelling by Hinzen (2010) also demonstrates such effects.

Reid (1910) studied this phenomenon, which was observed in the 1906 San Francisco earthquake, and pointed out that the observed rotations are too large to be produced by waves of linear elastic distortion. Such waves "*produce very small rotations, whose maximum amount, … is given by the expression* $2\pi A=\lambda$*, where A is the amplitude and* λ *the wavelength;*

with a wave as short as 10,000 feet (3 km) and an amplitude as large as 0.2 of a foot (6 cm), the maximum rotation would only be about 0.25 of a minute of arc [7.3 μrad], *a quantity far too small to be noticeable.*" (Reid, 1910, p. 44). A modern analysis of such rotational effects is presented in Todorovska and Trifunac (1990).

Observational seismology is based mainly on measuring *translational* motions because of a widespread belief that *rotational* motions are insignificant. For example, Richter (1958, footnote on p. 213) states that "*Theory indicates, and observation confirms, that such rotations are negligible.*" Richter provided no references (but perhaps after Reid, 1910, p. 44), and there were no instruments at that time sensitive enough to either confirm or refute this claim. Recent advances in rotational seismology became possible because sensitive rotational sensors have been developed in aeronautical and astronomical instrumentation.

2 Early attempts to study rotational motions

Ferrari (2006) summarized two models of an electrical seismograph with sliding smoked paper, developed by P. Filippo Cecchi in 1876 to record three-component *translational* motions and also the *torsional* movements from earthquakes. Although these instruments operated for several years, no rotational motion could be recorded because of low transducer sensitivity. Pioneers in several countries attempted to measure rotational motions induced by earthquakes. Nearly a century ago, Galitzin (1912) suggested using two identical pendulums installed on different sides of the same axis of rotation for separate measurement of rotational and translational motion. This was later implemented, for example, by Kharin and Simonov (1969) in an instrument designed to record strong ground motion. Using an azimuthal array of seismographs, Droste and Teisseyre (1976) derived rotational seismograms for rock bursts in a nearby mine. Inspired by Walter Munk, Farrell (1969) constructed a gyroscopic seismometer, and obtained a static displacement of <1 cm and a tilt of <0.5 μrad at La Jolla, California, during the Borrego Mountain earthquake of 09 April 1968 (magnitude 6.5) at an epicentral distance of 115 km.

Early efforts also included studies of explosions. For example, Graizer (1991) recorded tilts and translational motions in the near-field of two nuclear explosions using seismological observatory sensors to measure point rotations directly. Nigbor (1994) measured rotational and translational point ground motions directly with a commercial rotational micro-electro-mechanical system (MEMS) sensor and found significant near-field rotational motions (660 μrad at 1 km distance) from a one-kiloton explosion.

Rotations and strains of the ground and in the response of structures have been deduced indirectly from accelerometer arrays using methods valid for seismic waves having wavelengths that are long compared to the distances between sensors (e.g., Trifunac 1979; 1982; Oliveira and Bolt, 1989; Spudich et al., 1995; Bodin et al., 1997; Huang, 2003, Suryanto et al., 2006; Wassermann et al., 2009). The rotational components of ground motion have also been estimated theoretically, using kinematic source models (Bouchon and Aki, 1982; Wang et al., 2009) and linear elastodynamic theory of wave propagation in elastic solids (Lee and Trifunac, 1985, 1987). Recently, Graizer and Kalkan (2010) presented a history of strong motion seismology and rotations, outlining also future directions.

3 Techniques for measuring rotational motions

The general motion of the particles or a small volume in a solid body can be divided into three parts: translation (along the X-, Y-, and Z-axes), rotation (about the X- Y-, and Z-axes), and strain (six components). Figure 2(a) shows the axes in a Cartesian coordinate system for *translational velocity* measured by the usual sort of seismometers used in seismology, and Figure 2(b) shows the corresponding axes of *rotation rate* measured by rotational sensors (Evans and the International Working Group on Rotational Seismology, 2009). These are "body attached" coordinates, those that a seismic instrument would measure at a given instant as the sensors move and rotate through space. Converting an extended record of these body-fixed motions to recover motions in an Earth-fixed, quasi-inertial coordinate system has been performed for decades in "strapped down" inertial navigation systems such as those attached to a moving airplane. Lin et al. (2010) introduce these equations into seismology and earthquake engineering for recovering inertial-frame ground and structure motions.

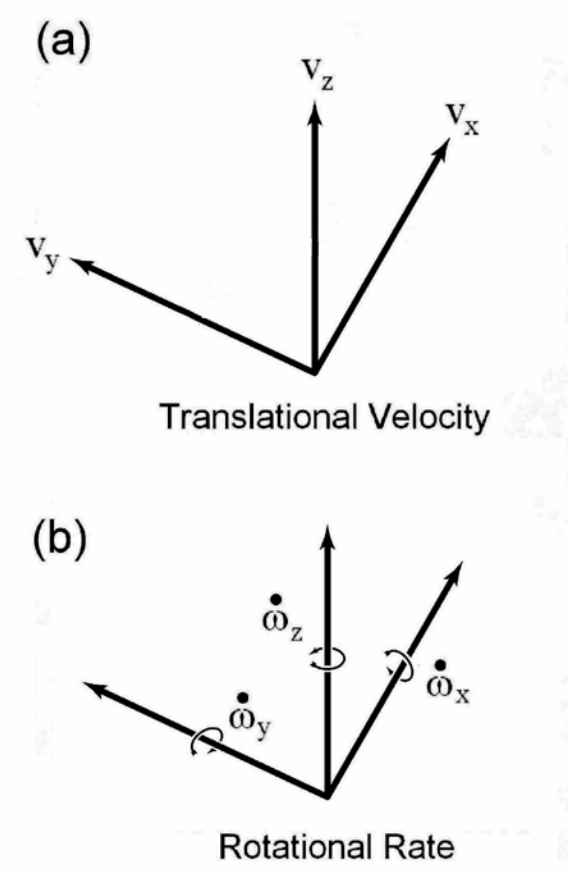

Figure 2 Coordinate system for translational velocity (adopted from Figure 1 of Evans and the International Working Group on Rotational Seismology, 2009). (a) Coordinate system for translational velocity. (b) Coordinate system for body-fixed or instantaneous rotational rate. This is the preferred nomenclature and sign conventions for observed translational and rotational motions in seismology and earthquake engineering. *X* and *Y* axes point into the page and are normally in the horizontal plane. Note the positions of rotation gyres with respect to the axes (the line in front breaks the line behind). Axes point in the positive directions of both the translational vectors and rotation vectors.

Annotations v and $\dot{\omega}$ are translational velocity (m/s) and rotation rate (rad/s); the subscripts x, y, and z refer to the X, Y, and Z components.

3.1 Theoretical basis

Rotational motion in seismology is usually formulated in the framework of linear elasticity theory with the assumption of *infinitesimal deformation* (Cochard et al., 2006). In a linear elastic medium the displacement **u** of a point **x** is related to a neighboring point **x**+**δx** by

$$\mathbf{u}(\mathbf{x}+\delta\mathbf{x}) = \mathbf{u}(\mathbf{x}) + \boldsymbol{\varepsilon}\,\delta\mathbf{x} + \boldsymbol{\omega}\times\delta\mathbf{x} \qquad (1)$$

where $\boldsymbol{\varepsilon}$ is the strain tensor and

$$\boldsymbol{\omega} = \tfrac{1}{2} \nabla \times \mathbf{u}(\mathbf{x}) \tag{2}$$

is a pseudo-vector representing the infinitesimal angle of rigid rotation generated by the disturbance. The three components of rotation about the X-axis, Y-axis and Z-axis are given by the following equations for such infinitesimal motions:

$$\begin{aligned} \omega_x &= \tfrac{1}{2} (\partial u_z / \partial y - \partial u_y / \partial z), \\ \omega_y &= \tfrac{1}{2} (\partial u_x / \partial z - \partial u_z / \partial x), \\ \omega_z &= \tfrac{1}{2} (\partial u_y / \partial x - \partial u_x / \partial y) \end{aligned} \tag{3}$$

Therefore, rigid rotations can be observed: (i) indirectly, by an array of translational seismometers for "cord" rotations associated with long wave lengths by assuming that contamination of translational signals by rotational motions is small, and that the linear elasticity theory is valid (e.g., Spudich and Fletcher, 2008), or (ii) directly, by rotational sensors for "point" body-fixed rotations (e.g., Lee et al., 2009b, and Lin et al., 2010).

Although classical elasticity theory works well for earthquakes in the *far* field recorded by vaulted seismographs, this linear theory may not be applicable in the *near* field. Theoretical work suggests that in shallow granular, cracked or biologically-disturbed, often dry continua (e.g., soil or weathered rock at or near Earth's surface), asymmetries of the stress and strain fields can create rotations separate from and larger than those predicted by classical elastodynamic theory (e.g., Teisseyre et al., 2006; 2008; Teisseyre, 2010). If so, these exaggerated rotations join previously known translational "site effects" for strong-motion stations. Further, unlike the traditional fault-slip model (Aki and Richards, 2002, p. 38-59) assuming a fault zone of *zero thickness*, Knopoff and Chen (2009) consider the case of faulting that takes place on a fault zone of *finite thickness*. They show that there is an additional single-couple term in the body-force equivalence and additional terms in the far-field displacement. They also show that the single-couple equivalent does not violate the principles of Newtonian mechanics because the torque imbalance in the single-couple is counterbalanced by rotations within the fault zone, with torque waves being radiated.

3.2 Measuring considerations

Most seismological instruments used in measuring translational ground motion are pendulum seismometers and accelerometers, and a tutorial on measuring rotations using multi-pendulum systems is given in Graizer (2009). It is important to note that pendulums are sensitive to translational motion and rotations. Horizontal pendulums are sensitive to the acceleration of linear motion, tilt, angular acceleration, and cross-axis excitations; and vertical pendulums are sensitive to the acceleration of linear motion, angular acceleration, and cross-axis excitations but not to tilt. Graizer (2005, 2010) provided complete equations of pendulum sensors used in seismology and their approximation for strong-motion seismology and also presented a method (Graizer, 2006) to extract residual tilt from uncorrected strong-motion accelerograms.

Measuring rotational ground motions is closely related to the traditional seismological observations of translational ground motions, and measurements of tilts and strains. However, it is beyond the scope of this Chapter to discuss tiltmeters and strainmeters. For these instruments, interested readers may consult, e.g., Agnew (1986), Segall (2010) and IS 5.1 by Zürn (2002) and in this NMSOP2.

4 Measuring rotational motions in practice

In the past decade, rotational motions from small local earthquakes to large teleseisms have been recorded successfully by sensitive rotational sensors in several countries (e.g., Takeo, 1998; McLeod et al., 1998; Igel et al., 2005, 2007; Suryanto et al., 2006; Cochard et al., 2006). In particular, the application of Sagnac interferometry in large ring-laser gyros provided greatly improved sensitivity to rotations at teleseismic distances and showed that the measured rotations are a good match to those estimated from linear elastic wave theory. Combined with translations, such rotational motions provide additional observations that lead to new approaches to the seismic inverse problem (Bernauer et al., 2009; Fichtner and Igel, 2009). Recently Igel et al. (2010) reported the first observations of Earth's free oscillations using ring laser recordings, and opened up potential applications of rotational seismology at long periods.

In contrast, strong-motion observations near the source in both Japan and Taiwan show that the amplitudes of these rotations can be one to two orders of magnitude greater than that expected from linear elasticity theory (e.g., Takeo, 1998; Lee et al., 2009b).

4.1 Ring laser gyros

An unexpected advance in studying rotational ground motions came from a different field of geophysics. Recent developments of highly sensitive ring laser gyroscopes to monitor the Earth's rotation also yield valuable data on rotational motions from large teleseismic events (Schreiber, 2009). The most important property that makes such rotation sensors useful for seismology is its very low noise floor and high sensitivity to rotational motions and its insensitivity to translational and cross-rotational motions. Very recently, the 3 September 2010 Canterbury, New Zealand earthquake (M_W 7.0) occurred near the Canterbury ring-laser station, which recorded many of the aftershocks (Schreiber, personal communication, 2010).

The rotation rates expected and observed in seismology range from the order of 10^{-1} rad/s (e.g., Nigbor, 1994; Trifunac 2009) for near seismic sources down to order 10^{-11} rad/s for large earthquakes at teleseismic distances (e.g., Igel et al., 2005, 2007). This range spans at least 10 orders of magnitude (200 dB), much as do translational motions, and it is unlikely that one instrument or one instrumental technology will be capable of providing accurate measurements over such a large range of amplitudes. Ring laser technology is currently the most promising approach to recording the small rotational motions induced by teleseisms, but to reach the sensitivities needed for seismic measurements large sizes (several square meters) are necessary and therefore the primary drawback of this technology is its very high cost.

4.1.1 Ring laser technology

Ring lasers detect the Sagnac beat frequency of two counter-propagating laser beams (Stedman, 1997; and Figure 3(c)), and Schreiber (2010) reviews the recent progress in ring laser technology. These active interferometers generally form triangular or square closed loops several meters across. The cavity is accurately evacuated and filled with a mixture of helium and neon for the laser, and the instrument is vacuum tight. If this instrument is rotating on a platform with respect to inertial space, the effective cavity length between the co-rotating and counter-rotating laser cavities differ and one observes frequency splitting

resulting in a beat frequency. This beat frequency δf is directly proportional to the rotation rate $\boldsymbol{\Omega}$ around the surface normal **n** of the ring laser system, as given by the Sagnac equation:

$$\delta f = \frac{4A}{\lambda P}\mathbf{n}\cdot\boldsymbol{\Omega}, \tag{4}$$

where P is the perimeter of the instrument, A its area, and λ the laser wavelength. This equation has three contributions that influence the beat frequency δf: (a) variations in the scale factor ($4A/\lambda P$) have to be avoided by means of a servo system which keep the perimeter of the ring constant; (b) changes in orientation **n** (tilting relative to Earth's rotation axis) enter the beat frequency *via* the inner product; and (c) variations in $\boldsymbol{\Omega}$ (e.g., changes in Earth's rotation rate and seismically induced rotations). The dominant contribution to δf is $\boldsymbol{\Omega}$. Note that translations do not contribute to the Sagnac frequency unless they affect P or A in some indirect manner. Next generation ring-laser gyro should have 3 axes attached to the same monument.

Ring lasers are sensitive to rotations only, assuming stable ring geometry and lasing. However, for co-seismic observations at the Earth's surface the horizontal components of rotation (i.e., tilts) will contribute to the vertical component of rotation rate (via **n** in Equation (4)**)**. As shown by Pham et al. (2009), the tilt-coupling effect is several orders of magnitude below the level of the earthquake-induced rotational signal unless one is very close to the source (where sensitive ring lasers would not be the appropriate technology; see next Section).

At present, there are ring laser gyros capable of measuring rotations induced by small local earthquakes or distant large teleseisms at four sites: 1.) Cashmere cavern, Christchurch, New Zealand (McLeod et al., 1998), 2.) Wettzell, Germany (Schreiber et al., 2005), 3.) Conway, Arkansas (Dunn et al, 2009), and 4.) Piñon Flat, California (Schreiber et al., 2009a). The ring laser gyros in these 4 sites all measure the vertical component of rotation rate (rotation about the vertical axis). However, measuring the horizontal components (rotations about horizontal axes) using ring laser technology is under development, e.g., VIRGO, Pisa, Italy (Di Virgillo, 2010).

4.1.2 G Ring laser and recording teleseisms

Since 2001, the "G Ring" laser (capable of measuring rotation rate of about 10^{-12} rad/s) has been operating at the primary geodetic station (Fundamentalstation) at Wettzell, in Bavaria (http://www.fs.wettzell.de/, last accessed 21 January 2011), along with many other geodetic instruments. A cross-sectional view of the site of the G Ring Laser is shown in Figure 3(a). The instrument is resting on a polished table consisting of a Zerodur™ disk (originally planned for a telescope) (Figure 3(b)) embedded in a 90-ton concrete monument. As shown in Figure 3(a), the monument is attached to a massive 2.7-m diameter concrete pillar and this is founded on crystalline bedrock 10 m below. A system of concrete rings and isolation material shields the monument and pillar from adjacent weathered-rock to eliminate its deformation and heat-flow contributions. The G Ring Laser is protected against external influences by a subsurface installation with passive thermal stability provided by a 2-m layer alternating between Styrofoam and wet clay, this beneath a 4-m soil mound. A lateral entrance tunnel with five isolating doors and a separate control room minimize thermal perturbations during maintenance. In addition the complete Zerodur™ table is covered by a

pressure tight casing which is lowered after maintenance - this results in a huge improvement of the signal/noise ratio.

After two years of thermal adaptation, the average temperature reached 12.2 °C with seasonal variations of less than 0.6 °C. Figure 3(c) shows the schematic drawing of instrument, and Figure 3(d) is a photo of the G Ring laser with its designer, Ulli Schreiber. The G Ring laser is large and sit on top of an impressive monument to reach extremely high sensitivity to study variations of the Earth's rotation. For seismological practice, a ring laser on top of a lighter monument will be adequate, as is the ring laser at Piñon Flat, California.

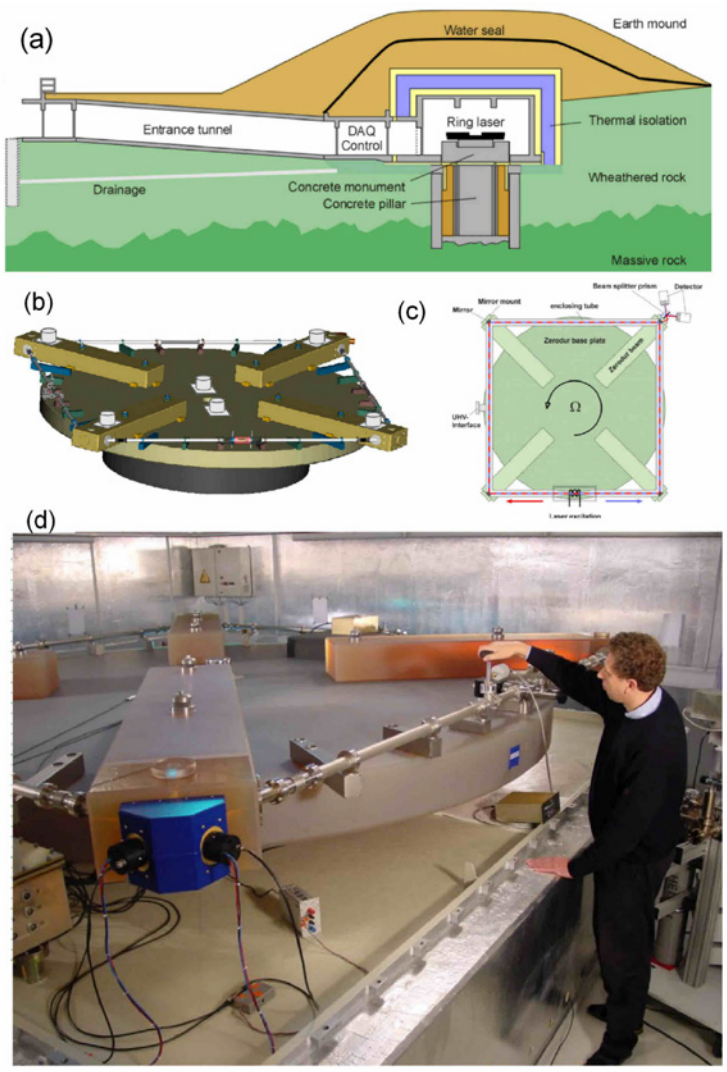

Figure 3 G Ring laser gyro at the Wettzell Superstation, Germany. (a) Cross-sectional view of the instrument site. (b) Instrument resting on a granite table. (c) Schematic drawing. (d) Photo of G Ring laser gyro with its designer, Ulli Schreiber.

Figure 4 is a comparison of direct point measurements of ground rotations around a vertical axis (red lines) to transverse accelerations (black lines, converted to rotation rate for each time window) for the M8.1 Tokachi-oki earthquake, 25 September 2003 (Igel et al., 2005). Figure 4(a) is a schematic view of the great-circle-path through the epicenter in Hokkaido, Japan, and the observatory in Wettzell, Germany. Figure 4(b–e) show the superposition of the rotation

rate derived from transverse translations (black) and measured directly (red) for various time windows: (b) the complete signal, (c) the latter part of the surface wave train, (d) the direct *S*-wave arrival, and (e) for the initial part of the surface wave train. These results confirm the expectation from linear elasticity that the waveforms of transverse acceleration and rotation rate (around the vertical axis) should be identical assuming plane harmonic waves. Information on subsurface structure is contained in the ratio between the corresponding motion amplitudes.

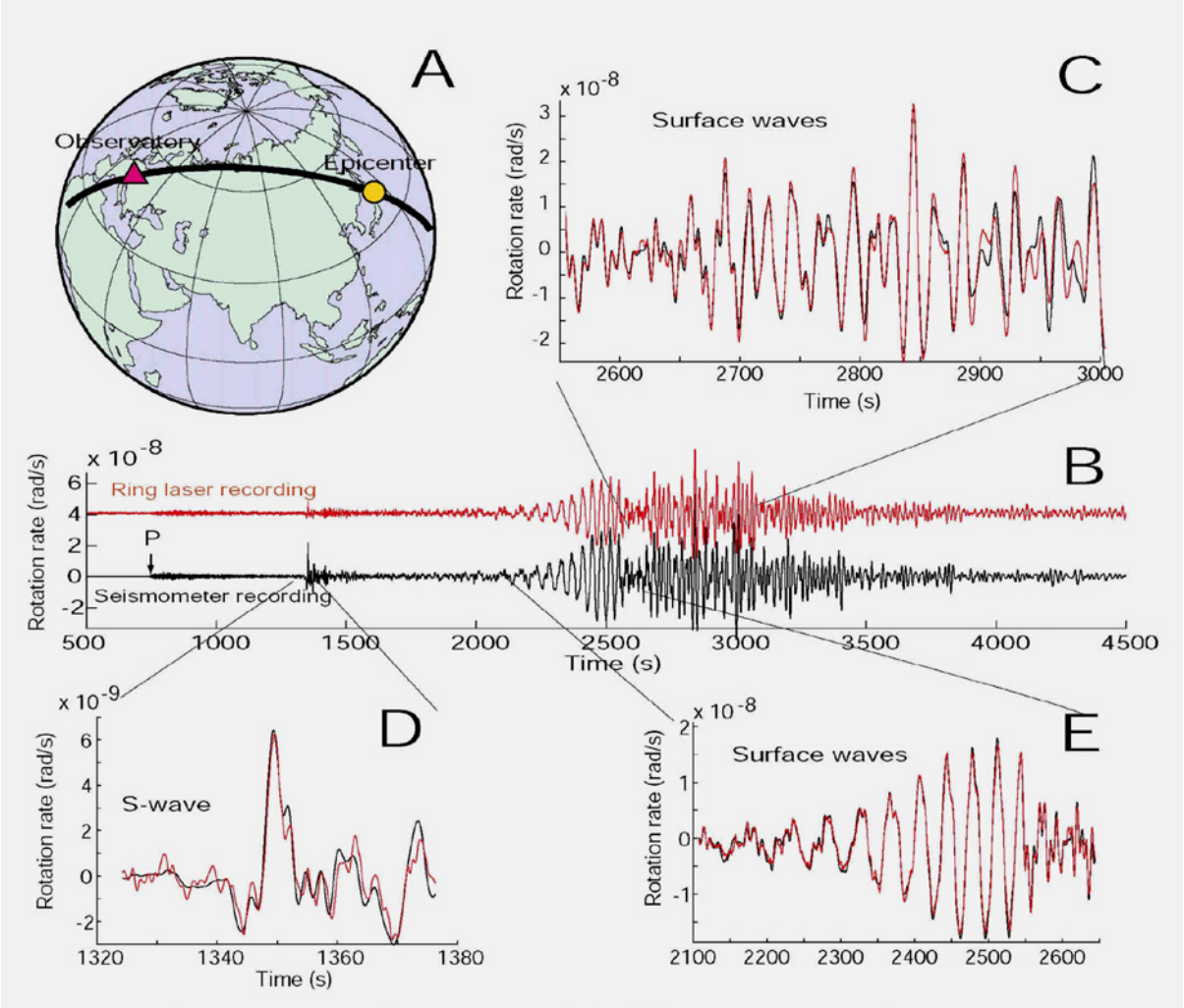

Figure 4 Comparison of direct measurements of ground rotational motions around a vertical axis (red lines) with transverse accelerations (black lines, converted to rotation rate for each time window) for the M8.1 Tokachi-oki earthquake, 25 September 2003 (after Igel et al., 2005).

4.2 Strong-motion inertial angular sensors

In aerospace, automotive, and mechanical engineering, smaller rotational-motion sensors are common and generically known as gyroscopic or inertial angular sensors. Nigbor (1994) used a MEMS-based Coriolis rotation-rate sensor to measure the rotational components of strong ground motions close to a large chemical explosion, and unsuccessfully attempted to resolve rotational earthquake motions in southern California for a decade. Similar sensors were used

by Takeo (1998) to measure rotational motions from an earthquake swarm ~3 km away. However, such sensors do not have the sensitivity to record rotations from small local earthquakes (magnitude ≈ 4) at distances of tens of kilometers.

4.2.1 The eentec™ Model R-1™ rotational seismometer

The eentec™ model R-1™ rotational seismometer is the first modestly-priced (about US$5,000 each) three-component sensor capable of recording small earthquakes at distances up to several tens of kilometers. It uses electrochemical technology in which the motion of an electrolytic fluid inside a torus is sensed electronically, yielding a voltage signal proportional to rotational velocity. (For more information on this pioneering transducer principle see Vol. 1, Chapter 5, subsection 5.3.10). Nigbor et al. (2009) carried out extensive tests of commercial rotational sensors and concluded that the R-1 sensor generally meets the specifications given by the manufacturer but that clip level and frequency response vary from those specifications and between individual channels enough that more detailed calibrations are warranted for each unit. A typical transfer function for the R-1 can be found at the manufacturer's website (http://www.eentec.com/, last accessed 21 January 2011). The instrument response is roughly flat from 0.05 to 20 Hz and its self noise (rms) is <10 µrad/s over the same frequency band.

Schreiber et al. (2011) conducted a comparison test of an R-1 rotational seismometer and a fiber optic gyro µFORS (Litef GmbH) at the facility of Physikalisch-Technische Bundesanstalt (PTB) in Germany (Department "Längen- und Winkelteilungen"). The two sensors were co-located at the rotation turn table that allows the precise measurements of the revolution angles and provides the time marks for calculation of the rotation rate. The authors found that the R-1 could not adequately detect low-frequency variations of rotation rate, but at frequencies above 0.1-1 Hz, its signal was quite similar to that of the µFORS. They concluded that "*The declared accuracy characteristics of R-1 are [according to the manufacturer, the] following: frequency bandwidth 0.033-50 Hz, resolution* 1.2×10^{-7} *rad/sec, clip level 1 rad/sec. According to our tests, the resolution, or minimal detectable rotation rate change is about* 2×10^{-5} *rad/sec, and the clip level is* 2.5×10^{-2} *rad/s.*" Moreover, as found by Joachim Wassermann (personal communication, 2011), the R-1 rotational seismometer is very sensitive to temperature. The overall gain changes with increasing temperature, measured from 15 to 50 °C, by a factor of at least 30%.

The R-1 rotational seismometers recorded several hundred local earthquakes and two explosions in Taiwan (Lee et al., 2009b). The top panels in Figure 5 show the instruments deployed at station HGSD in eastern Taiwan (Liu et al., 2009). Figure 5(a) is a schematic drawing of the various seismic, geodetic, and strain instruments there, and Figure 5(b) shows the subset of the instruments deployed in the shallow vault at the left hand side of the upper drawing. These instruments include a data logger (Quanterra Q330), an accelerometer (Kinemetrics Episensor), a six-channel digital accelerograph (Kinemetrics K2 with an external rotational seismometer, R-1 by eentec), and a short-period seismometer (Mark Products L-4A). The K2+R-1 instrument is at the left hand side, and the yellow-color box is the R-1 rotational seismometer.

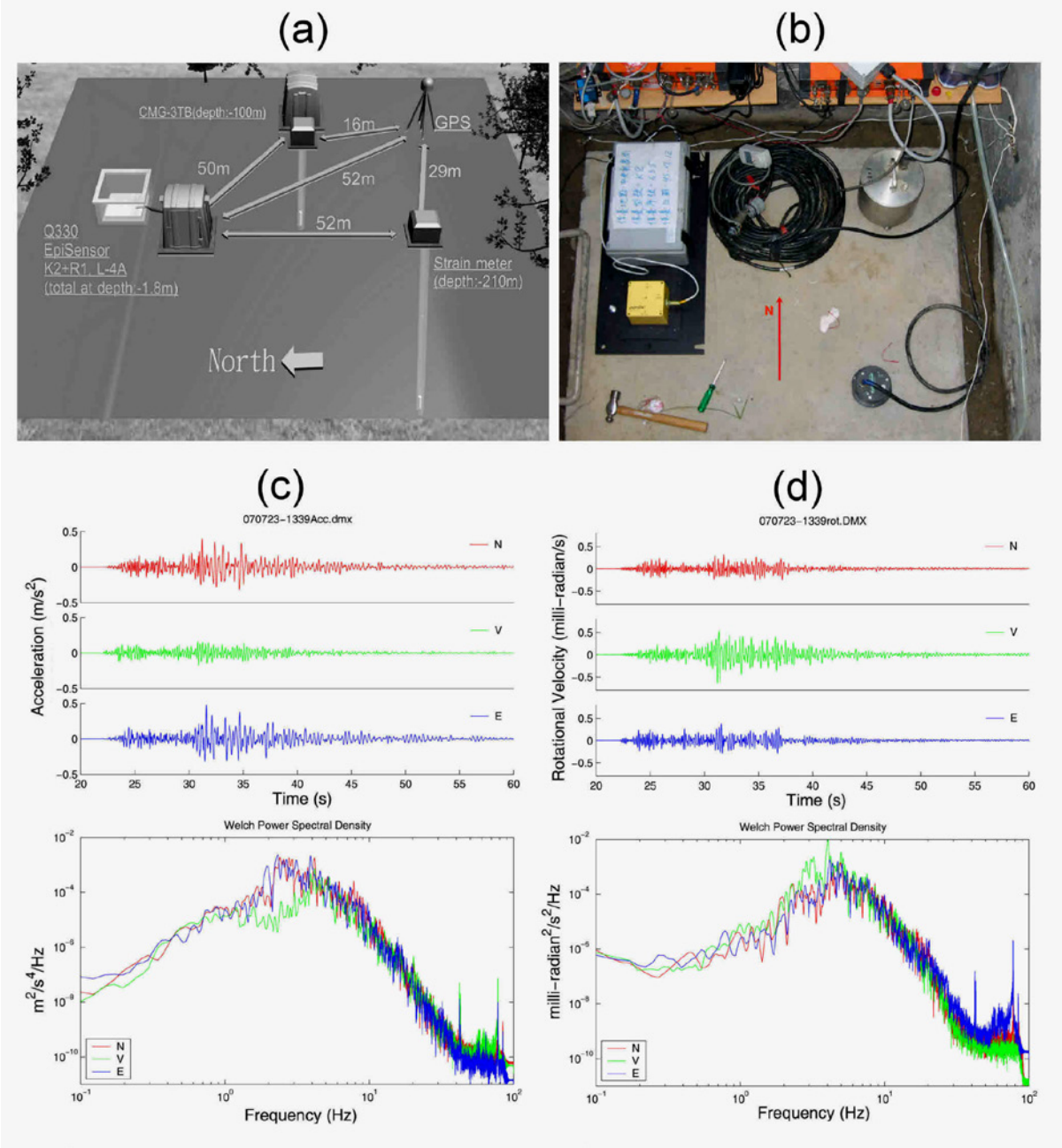

Figure 5 (a) Schematic of instrument layout at station HGSD in Taiwan. (b) Photo showing the instrument vault containing a K-2 accelerograph (upper left), an R-1 rotational seismometer (yellow box), an EpiSensor accelerometer (lower right-hand side), and an L-4A short-period velocity seismometer (upper right-hand side). (c) Recorded translational accelerations (upper panel) and their spectra (lower panel) from an M_W 5.1 earthquake 51 km from this site. (d) Recorded rotational rates (upper panel) and their spectra (lower panel) from the same earthquake.

The largest peak rotational rate recorded at the HGSD station (to early 2008) is from an M_W 5.1 earthquake at a hypocentral distance of 51 km at 13:40 UTC, 23 July 2007. Figure 5(c) shows the amplitudes and spectra of translational accelerations recorded by the K2's accelerometer. The peak ground acceleration was 0.47 m/s^2 (4.8% g) and the two horizontal components have much higher peak amplitude than the vertical. Figure 5(d) shows the amplitudes and spectra for rotational rates recorded from the external R-1 seismometer. The

peak rotational rate was 0.63 mrad/s for the vertical component, which is more than twice the rotational rate recorded on either of the horizontal components. The dominant frequency band in ground acceleration is about 2–5 Hz (horizontal components), whereas for the ground rotation rate it is about 2.5–5.5 Hz for the vertical component. Other studies report observations made with the R-1 sensor and compare these point measurements of rotation to array-derived area rotations (e.g., Wassermann et al., 2009).

A new model, the R-2™, became available from eentec in 2010. As of this writing, laboratory tests on twelve R-2 units indicated that their performance did not meet the technical specifications given by the manufacturer, though the design itself appears sound (Evans et al., 2010). Other promising efforts to develop new rotational sensors include that of Northrop Grumman Litef GmbH, Freiburg, Germany, which is developing a rotational sensor specifically for seismological applications and based on fiber optic gyroscope principle, and that of ATA Sensors (Smith, 2010), which is applying an entirely different technology to develop sensors for weak motion (using a solid proof mass) and for strong motion (using their existing patented magneto-hydrodynamic, or MHD, technology).

4.2.2 Laboratory calibration of rotational sensors

Most rotational sensors output a signal proportional to rotational velocity but a few produce rotational acceleration. In either case the only natural reference signal commonly available is the Earth's rotation about its pole, which is about 73 μrad/s about the North Pole (right-handed rotation vector pointing north). While the Earth's rotation is a very useful calibration signal for weak-motion rotational sensors such as large-area ring-laser gyroscopes, it is near or below the noise level of many existing strong-motion sensors, and so is effectively unavailable for their calibration. Further, Earth rotation is a roughly 0-Hz signal ("DC"), and thus it is not useful for establishing any rotational sensor's linearity or transfer functions. Thus, strong-motion rotational sensors require the use of a precision rotational shake table, and these are costly. In what follows, we focus on calibration of strong-motion rotational sensors for which the Earth's rotation is not a viable proof signal.

In all cases, operators are advised to use a right-handed set of axes including right-handed definitions of rotational pseudovectors (e.g., *Evans* et al., 2009, their Figure 1). Note, of course, that many seismic instruments record in the channel order Up, North, East; so *x* should be thought of as East, *y* as North, and *z* as Up for the sensor to be right handed.

IEEE Standard 671-1985 (1985) provides useful guidance, while procedures specific to seismic rotational instruments are in development and will draw on both this standard and experiences at several laboratories in the early years of testing such instruments. At present, the primary concerns of those laboratories are the transfer function (response function) of rotational sensors, the self-noise levels of these sensors, and the cross-axis terms, including both rotation-to-rotation and translation-to-rotation cross-axis sensitivities. Existing works on testing rotational seismic sensors include Nigbor et al. (2009), Evans et al. (2010), Schreiber et al. (2011), and various private reports of sensor testing by the laboratories active in this field.

Transfer function. Early rotational-velocity sensors for strong-motion work have proved to be less than flat in response and to vary even in mid-band sensitivity by far more than the 1% industry norm for sensitivity accuracy. Thus, it is essential that all such sensors be calibrated individually on a shake table to determine amplitude and phase responses, from which

Laplace poles and zeros may be estimated by a parametric fit. In practice, this calibration proceeds by inputting known sine wave motions on axis with the sensor under test, and that intervals of at least three cycles of each sine frequency (preferably many more) be recorded and compared to these known inputs. Alternatively, a slowly swept sine wave spanning the same frequency band may be used. This test generally should proceed at half-octave steps in frequency from one octave below the low-frequency corner of the sensor to one octave above its high-frequency corner (some shake table systems cannot drive the sensors to this peak frequency, but one should get as high as possible without damaging the table). The sensor output and the input motions must be recorded on a common time base (ideally with simultaneous sampling to within about 10 μs) in order to recover phase accurately. In practice, it is common to use either the positional feedback of the shake table or a reliable reference sensor to measure this input motion, so the resulting transfer function is relative to this reference signal. Empirical evidence suggests that amplitude response is best measured by comparing peak power between PSDs of the test and reference traces while phase appears to be most stably measured by cross correlation of the traces. In co-testing different instruments one should keep them near and at the same distance from the rotation point of the table to limit centrifugal inputs.

Self noise. At present, strong-motion rotational sensors appear to have self noise levels well above Earth's ambient rotational seismic background motions. The level of rotational Earth noise is not very well known at present. However, the absence of microseism-band increases in typical instrument-noise figures argues against a significant Earth-noise input. Thus, the single-sensor method of *Evans* et al. (2010) may be used until sensor noise levels drop and sensitivities rises (The same will not be true for weak motion sensors.) When that stage of sensor development is reached, there is no reason in principal not to use the two- or three-sensor methods described in that paper and works cited therein. The single-sensor method is to record sensor output with a sensitive recorder at some quiet location during a quiet interval, generally overnight. One computes the PSD and simply attributes all of it to sensor self noise. Details of a "standard" method for this computation and subsequent "operating range diagram" representation of sensor noise are given by Evans et al. (2010).

Rotation-to-rotation cross-axis sensitivity. Industry norms for translation-to-translation and rotation-to-rotation cross-axis sensitivities are typically about 1%. For example, a 1-g input to a translational accelerometer oriented at right angles to that input acceleration should register no more than 0.01 g in response. The unit "g" means Earth surface gravitational acceleration, typically about 9.8 m/s^2. It is a unit preferred by the earthquake engineers. This 1% norm is reasonable for seismology and earthquake engineering applications as well. That is, a rotation rate of 1 mrad/s should register on the orthogonal components as no more than a 10 μrad/s output signal. In most sensors, imperfect alignment between the sensor case and the true active axes of the sensor dominate this cross-axis term (1% corresponds to an alignment error of about 0.6°).

Translation-to-rotation cross-axis sensitivity. It can be difficult to compare motions with differing units and fundamental physics, in this case translation and rotation, but there is a simple method that accounts for the wide anticipated use of rotational sensors for correcting tilt-induced errors in horizontal translational sensors. Tilt within Earth's gravitational field applies ~1 μg of acceleration to horizontal translation sensors for every 1 μrad of tilt., This is a first-order sensitivity in the presence of any significant rotational motions. Thus, one should compare the output of a rotational sensor excited by translational input motions to the true translational inputs *via* $g\sin\theta$, where g is local gravitational acceleration and the translational sensor is rotated by an angle of θ about a horizontal axis (i.e., tilted). Angle θ is generally

obtained by integrating rotational velocity to rotation angle in a collocated rotational sensor. Because rotational motions in earthquakes are relatively small, perhaps 1 to 10% of translational motions when so compared, the translation-to-rotation cross-axis sensitivity of rotational sensors must be well under one part per thousand (1 PPT) in order to correct the translational sensors accurately. A similar level of immunity to translational motions is needed to make reliable use of rotational data for other purposes, such as single-site computation of surface-wave phase velocity or reducing the size of response kernels in seismic tomography. This restriction is quite stringent but has been met by well designed sensors.

4.2.3 Field deployment of rotational sensors

Field deployment of rotational sensors requires site selection and preparation similar to that for any seismological instruments (Trnkoczy, et.al., 2002 and also Chapter 7 in NMSOP2). The R-1 rotational seismometer can be connected to a data logger, as with any other analog-output seismic sensor. An earlier approach in Taiwan was to connect the R-1 to a six-channel accelerograph (Kinemetrics model K2) forming a six-degree-of-freedom (6-DOF) self-contained instrument. In this case, the K2 and R-1 are mounted together on a thick metal plate. A vault was constructed at the HGSD station to house this K2+R1 instrument. In addition, a six-channel, 24-bit Quanterra Q330 data logger was deployed to record ground acceleration using a Kinemetrics EpiSensor and to record ground velocity using a Mark Product short-period seismometer (Model L-4A; 2 Hz natural frequency). Instruments in operation during the Phase 2 operation of Liu et al. (2009) have been shown in Figure 5 above.

Another configuration used in Taiwan is to connect an R-1 rotational seismometer directly to a 24-bit Quanterra Q330 datalogger. Data are telemetered from the field to the Institute of Earth Sciences in Taipei in real time at 20 sps (samples per second), and continuous data are also recorded on an external hard disk in the field at 100 sps, The disk is collected every three to four months when the station is being serviced. Figure 6 (on next page) shows an installation of broadband seismometer, accelerometers, and rotational sensor at the Ninganchiao station (NACB) operated by the Institute of Earth Sciences, Academia Sinica, Taiwan. Station NACB is near the back of a 60-m tunnel into a hill composed of marble, and is located at 24.1738º N, 121.5947º E, and 130 m above the sea level. This station was established in 1995 as one of the Broadband Array in Taiwan for Seismology (BAT) stations (http://bats.earth.sinica.edu.tw/, last accessed 21 January 2011). In April, 2008, a Model R-1 rotational seismometer of eentec and an accelerometer (Model TSA-100S of Metrozet) were installed at this site. This set of instruments forms the NAC1 station and is recorded by a 6-channel Q330 datalogger of Quanterra. In 2010, the Metrozet accelerometer was replaced by a Model AGI 520 tiltmeter.

5 Discussion of results and benefits of studying rotational motions

Many authors have emphasized the benefits of studying rotational motions (e.g., Twiss et al., 1993; Spudich et al., 1995; Takeo and Ito, 1997; Teisseyre et al., 2006; Trifunac, 2006; Igel et al., 2007; Fichtner et al., 2009; and Teisseyre, 2010), and its relevance to engineering applications (e.g., Trifunac, 2009; Castellani and Guidotti, 2010). Rotational seismology is also of interest to physicists using Earth-based observatories for detecting Einstein's gravitational waves (e.g., Lantz et al., 2009) because they must correct for the underlying

Earth motion (e.g., DeSalvo, 2009; Di Virgilio, 2010). Here we briefly discuss some basic issues.

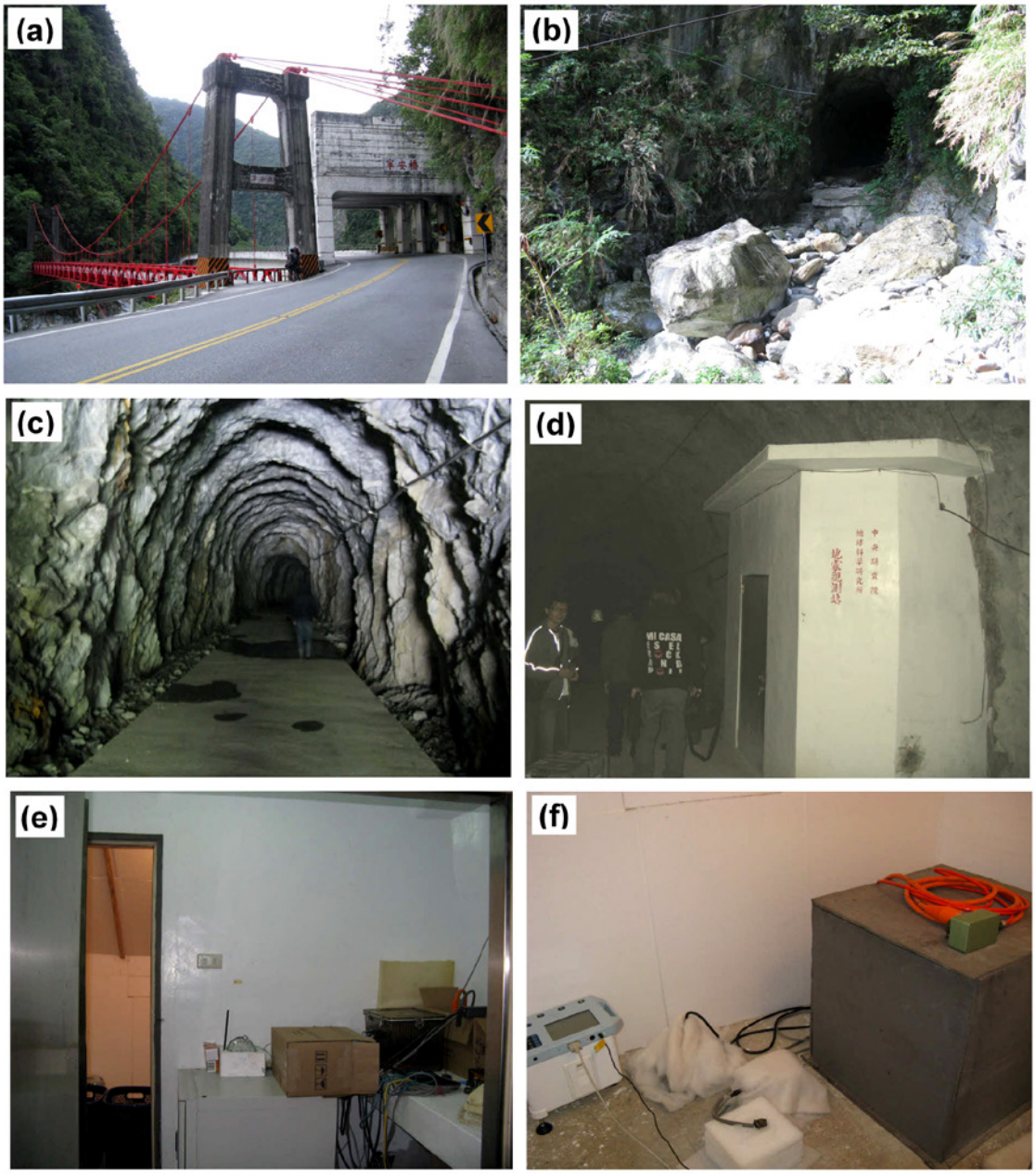

Figure 6 Photos of an installation of broadband seismometer, accelerometers, and rotational sensor at the Ninganchiao station (NACB) operated by the Institute of Earth Sciences, Academia Sinica, Taipei, Taiwan: (a) The Ningan Bridge in the National Park northwest of Hualien, Taiwan, (b) the entrance to a tunnel near the Ningan Bridge, (c) the tunnel of about 60 m, leading to the Ninganchiao station, (d) the front entrance of the Ninganchiao station, (e) the recording room, showing a 6-channel Q330HR recorder to the right and the entrance to the instrument room, (f) the STS-2 broadband velocity seismometer, which is enclosed in a metal box to the right, together with two accelerometers (Model Episensor ES-T of Kinemetrics, and Model TSA-100S of Metrozet) in the middle (covered by insulation material), and a Model R-1 rotational seismometer of eentec near the bottom to the left (also covered by insulation material).

5.1 Linear and nonlinear elasticity

Real materials of the Earth are heterogeneous, anisotropic, and nonlinear, especially in the damaged zones surrounding faults and in poorly consolidated sediments, soil, and weathered, fractured rock near the surface. These characteristics are typical of site conditions just beneath seismic instruments, particularly for strong-motion instruments that are intended to record the sort of motions experienced by shallow-foundation structures, and in consequence, commonly are placed on the surface. In the presence of significant nonlinearity we are forced to consider the mechanics of chaos (Trifunac, 2009), and we must record both the rotational and translational components of strong motion in order to interpret such complexities.

Seismology is primarily based on the classical, linear elasticity theory, which is applicable to simple homogeneous materials under infinitesimal strain. "Cord" rotation is defined for such materials as the curl of the displacement field in Equation (2), and in this classical elasticity theory, the rotational components of motion are contained in the S waves. Meanwhile, continuum mechanics has advanced far beyond such classical theory. In particular, the elasticity theory of the Cosserat brothers (Cosserat and Cosserat, 1909) incorporates both a local rotation of continuum particles and the translational motion assumed in classical theory, as well as a couple stress (a torque per unit area) in addition to the usual the force stress (force per unit area). In the constitutive equation of classical elasticity theory for an isotropic material there are two independent elastic constants, while in Cosserat elastic theory there are at least six elastic constants. Pujol (2009) provides a tutorial on rotations in the theories of finite deformation and micropolar (Cosserat) elasticity. Twiss (2009) derives an objective asymmetric micropolar moment tensor from a discrete-block model for a deforming granular material. He also investigates seismogenic deformation associated with volumes of distributed seismicity in three different geographic areas, and finds support in the micropolar model for the effects of a granular substructure on the characteristics of seismic focal mechanisms.

Angular squeeze strain deformations were found by Gomberg and Agnew (1996) for all earthquakes they studied on the basis of their experimental strainmeter data. Such squeeze circular deformations cannot be explained in a frame work of the classical continuum theory, and therefore, the authors attributed such founding to some systematic errors. However, as pointed out by Roman Teisseyre (personal communication, 2011), these deformation may exist without such errors according to the asymmetric continuum theory (Ayden et al., 1993; Teisseyre, 2010).

5.2 Near-field seismology

Although the observed rotational motions for teleseisms recorded in a rock vault agree well with estimates based on the classical elasticity theory (e.g., Igel et al., 2005; 2007), this is not the case for local earthquakes recorded by strong-motion installations. As first noted by Takeo (1998) and later confirmed by Lee et al. (2009b), observed rotational rates from local earthquakes are much larger than those predicted by the classical elasticity theory. For example, Bouchon and Aki (1982) determined theoretically that a maximum rotational rate of 1.5 mrad/s is expected for an M6.5 earthquake, whereas maximum rotational rates exceeding 1 mrad/s have been observed for much smaller (M4.5–5.5) earthquakes in Japan and Taiwan, for which the classical elasticity theory predicts far smaller rotations. Takeo (1998) reported the largest rotational rate to be 26 mrad/s around the north-south horizontal axis from the second largest earthquake (M5.2 at 14:09 UTC, 03 March) during the 1997 swarm, east of Cape Kawana, offshore Ito, Japan (epicentral distance ~3 km). As of the end of 2009, the

largest rotational rate recorded at the HWLB station (Hualien, Taiwan) was 2.58 mrad/s around the east-west horizontal axis for an M_W 6.4 earthquake offshore that occurred at 13:02 UTC on 19 December 2009, and was located offshore at a hypocentral distance of about 49 km. The peak rotational rate was 1.57 mrad/s around the north-south axis, and 0.68 mrad/s around the vertical axis. The corresponding peak ground accelerations were 1.16, 1.85, and 0.50 m/s^2 for the east-west, north-south, and vertical component, respectively (5.1–18.9% g).

Figure 7 shows the vertical-axis peak rotational rate versus horizontal-axis peak ground acceleration for the earthquake data set from Takeo (2009) (top frame), and for the earthquake data set (22 August 2008 to 25 December 2009) recorded (at different distance ranges) at station HWLB, Taiwan (bottom frame; N is the number of data points).

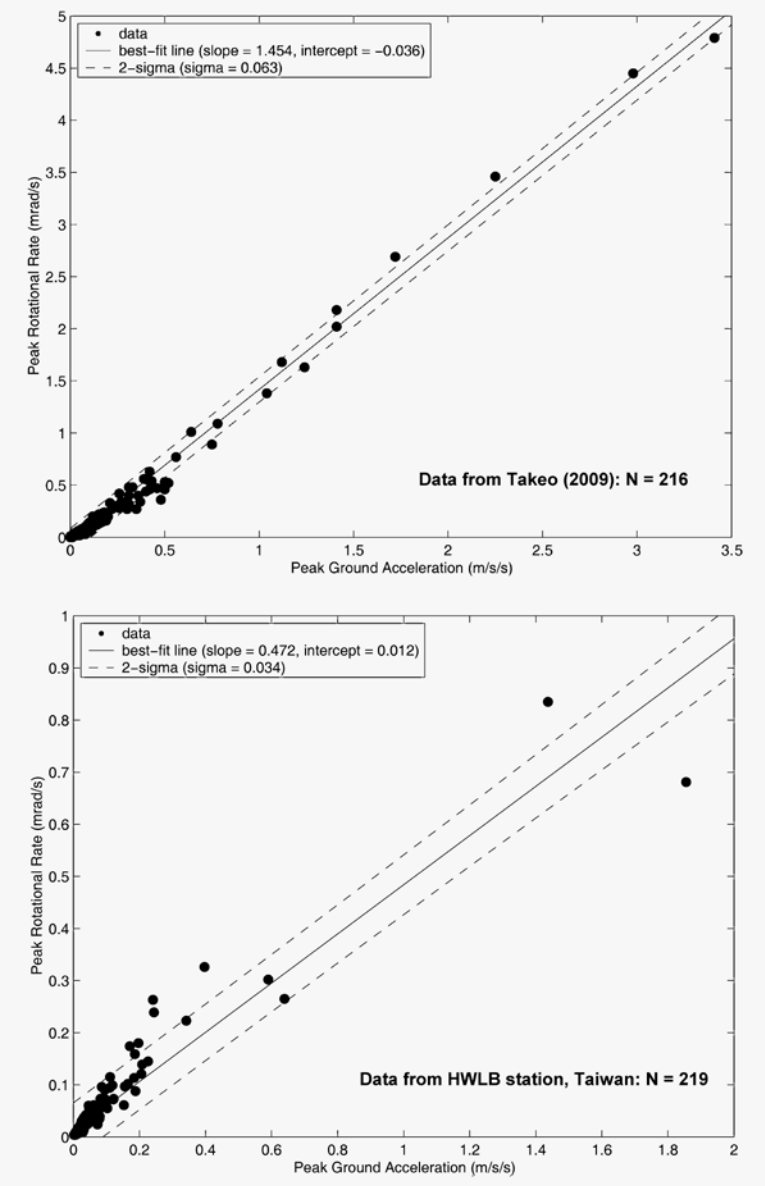

Figure 7 Vertical peak rotational rate (PRR) versus horizontal peak ground acceleration (PGA) for the earthquake data set from Takeo (2009) (**top frame**), and for the earthquake data set (22 August 2008 to 25 December 2009) recorded at the HWLB station, Taiwan (**bottom frame**). N is the number of data points. Best-fit lines are determined using linear least-squares. Note the difference in the scaling of the axes for the two plots.

The slopes for the two data sets (1.454 versus 0.472) are significantly different. But, as noted below, this may reflect a difference in site conditions. While the Taiwan data appears to exhibit more scatter than in the Takeo (2009) data, its variance actually is only about half. One should also note that the range of the observations in the two plots is significantly different, which may account, at least in part, for the difference in scatter. Whereas the earthquake sources for the Takeo (2009) data belong all to a compact, nearby swarm, the Taiwan data relate to widely separated earthquake sources. Several authors have noted similar linear relationships (e.g., Spudich and Fletcher, 2008; Stupazzini et al., 2009; Takeo, 2009; and Wang et al., 2009). In particular, Takeo (2009) showed "*a linear correlation between the maximum rotational displacements around vertical axis and the maximum* [ground] *velocities*". The two plots in Figure 7 are equivalent to Takeo's linear relationship, without the need to perform the integration for the measured rotational rate and ground acceleration to obtain rotational displacements and ground velocities. The linear slope in Figure 7 has units of s/km, i.e., of slowness. Spudich and Fletcher (2008) interpreted this "slowness" as the inverse of an "apparent velocity", characterizing the seismic wavefield beneath the recording station.

Spudich and Fletcher (2008) computed peak values of ground strain, torsions, and tilts for the 2004 Parkfield earthquake (M_W 6.0) and four of its aftershocks (M_W 4.7–5.1) using the data recorded by the UPSAR array of accelerators. The observed peak horizontal acceleration and velocity were 0.45 g and 27 cm/s during the mainshock, and derived a maximum rotation rate of 1.09 mrad/s for the vertical component, which agrees well with the theoretical result of Bouchon and Aki (1982) mentioned above. Takeo (2009) noted that his observations of peak rotation values in the near-field region during an 1998 earthquake swarm offshore Ito, Izu Peninsular, Japan, are much larger than those calculated by Spudich and Fletcher (2008), and he proposed the following explanations: the different spatial scale of rotational motion measured by a single point gyro measurement and by an array observation (that is, the point observation not benefiting from averaging out local site variations), the effects of topography, and the difference of the degree of geologic maturation between the San Andreas fault and the swarm volume offshore Ito. Two arrays of both rotational and translational sensors have been deployed by Wu et al. (2009) in Taiwan to study this discrepancy.

5.3 Using explosions to study rotational motions

Because large earthquakes rarely occur near existing seismic stations, explosions have been used by several pioneers to study rotational motions (e.g., Graizer, 1991; Nigbor, 1994). Lin et al. (2009) deployed an array of eight triaxial rotational sensors, 13 triaxial accelerometers, and 12 six-channel, 24-bit data loggers with GPS time receivers to record two explosions in northeastern Taiwan. These instruments were installed at about 250 m (1 station), 500 m (11 stations), and 600 m (1 station) from the explosions. The group of 11 stations forms a "Center Array" with station spacing of about 5 m. The code name for the first shot with 3,000 kg explosives is "N3P", and that for the smaller second shot (750 kg) is "N3". Although the N3P shot used four times as much explosive as shot N3, the peak ground translational acceleration and rotational rates at all 13 station sites for N3P are only about 1.5 times larger than that for N3, suggesting some nonlinear process. Large variations (by tens of percent) in translational accelerations and rotational rates were observed within the small Center Array. The largest observed peak rotational rate was on the horizontal transverse component at 2.74 and 1.75 mrad/s at a distance of 254 m from the N3P and N3 shots. As pointed out by Joachim Wassermann (personal communication, 2011), this experiment may have problems with strain-tilt coupling that Lin et al. (2009) did not consider.

The acceleration data from these two explosions were used by Langston et al. (2009) to compute acceleration spatial gradients, horizontal strains and horizontal rotations, and to perform a radiometric analysis of the strong ground motion wave train. The analysis yields a complex, frequency-dependent view of the nature of seismic wave propagation over short propagation distances that imply significant lateral velocity changes in the near-surface crustal structure. Areal strain and rotation about the vertical have equal amplitudes and suggest significant wave scattering within the confines of the river valley where the experiment was performed and/or significant departure from an axisymmetric explosion source. Gradiometry shows that the P wave arrives at the array 35 degrees off-azimuth clockwise from the straight-line path and appears to have been refracted from the northern side of the valley (the shots are west of the Center Array). Chi et al. (2011) successfully recovered the first order features of vertical rotation-rate ground motions from the translational velocity waveforms in the frequency band 0.5–20 Hz by using the software of Spudich and Fletcher (2009); they deduced strain as large as 10^{-4}. To fulfill the uniform-rotation assumption in the linear elasticity theory, one must use a small-aperture array. However, inverting data from an array of small spatial dimension requires accurate waveforms of high signal-to-noise ratio and high sampling rates. Since waveforms from adjacent stations are very similar, low levels of noise can have a strong influence on estimated displacement gradients. The recordings of Lin et al. (2009) were limited to 200 samples per second (sps). However, much higher sampling rates are required in the near field recording of explosions, which also radiate rather high-frequency (>100 Hz) waves.

5.4 Processing collocated measurements of translations and rotations

Processing collocated observations of rotation and translation is routinely performed in the inertial navigation units of aircraft and other vehicles. A similar analysis is possible for various combinations of strain components, rotations, and translations in seismology and earthquake engineering. With the exception of velocity-strain combinations (e.g., Gomberg and Agnew, 1996) these methods were largely unexplored until the recent work of Lin et al. (2010). Lin et al. demonstrated an appropriate set of these equations for earthquake engineering and seismology, and used them to recover inertial-frame displacements and rotations. Further, it is already apparent that rotational motions provide useful additional analysis opportunities — simply put, more data at a site yield more results:

Phase velocities and propagation directions. A simple calculation for non-dispersive linear-elastic plane waves with transverse polarization shows that the ratio of transverse acceleration to vertical-axis rotational velocity is proportional to local phase velocity. This result implies that information on subsurface velocity structure (otherwise only accessible through seismic array measurements and combined analyses) is contained in any single-point measurement that includes rotational sensors. It has been shown that such ratio-derived phase velocities agree with velocities predicted by theory (Igel et al., 2005; Kurrle et al., 2010). In a recent theoretical study based on full ray theory for Love waves (normal mode summation) Ferreira and Igel (2009) demonstrated that the Love wave dispersion relation also can be obtained by taking the spectral ratio of transverse acceleration to vertical-axis rotation rate. This result implies that seismic surface wave tomography is possible without requiring sub-arrays to determine local mean phase velocities. Information on the direction of propagation also is contained in the azimuth-dependent phase fit between rotations and translations. Since this fit is optimal in the direction of propagation the back azimuths can be estimated to within a few degrees (Igel et al., 2007). Linking observational translations, strains, and rotations together

also is advocated by Langston (2007) to yield a snapshot of the wavefield including direction, slownesses, and radial/azimuthal amplitude gradients independently at each such station.

Towards a new kind of tomography. The possibility of deriving local dispersion relations from single-station records leads to the question of what subsurface volume one resolves and to what degree depth-resolution velocity perturbations can be recovered. The method of choice to answer this type of question is the adjoint method (Fichtner and Igel, 2009), with which sensitivity kernels (first Fresnel zones) can be calculated to indicate the volume in which the observable parameters (typically travel times) are sensitive to structural perturbations. Fichtner and Igel (2009) introduced a new observable quantity — apparent shear wave velocity — which is a time-windowed ratio of the moduli of translational velocity and rotation angle. It turns out that sensitivity near the source vanishes, leading to a new type of resolution kernel with high sensitivity only in the vicinity of the receiver and in a somewhat smaller portion of that volume than the kernels of translational motions alone. This result implies that a superior tomographic inversion for near-receiver structures based on rotations and translations is possible. Synthetic tomographic inversions of this kind are given in Bernauer et al. (2009).

Scattering properties of the crust: Partitioning of P and S waves. The partitioning of P and S energy and stabilizing the ratio between the two is an important constraint on the scattering properties of a medium. Igel et al. (2007) discovered surprisingly great rotational energy in a time window prior to teleseismic S, belonging to the P-wave coda. Detailed analysis of the signals and modelling of wave propagation through three-dimensional random media demonstrate that these signals can be explained with P–SH scattering in the crust with scatterers of roughly 5-km correlation length and rms perturbation amplitude of 5% (the latter is better constrained). Additionally, rotation measurements can be used as a filter for SH type motion (Takeo and Ito, 1997). These results further illustrate the efficacy of rotation measurements in their own right.

6 Conclusions

Seismology has been very successful in vaults in the *far field* because classical elasticity theory works very well for interpreting recorded translational motions of bedrock at large distances. Because of this success and limited instrumentation options, most funding for earthquake monitoring historically has gone into global and regional seismic networks using only translational seismometers. However, to improve our understanding of damaging earthquakes we must also deploy rotational and translational instruments in the *near field* of active faults where potentially damaging earthquakes (magnitude > 6.5) occur *infrequently*. For strong-motion seismology and engineering, this requires long-term commitment to monitoring because a damaging earthquake on any given fault may not take place for hundreds of years. Given that financial resources are often limited, recording ground motions in the near field would require extensive seismic instrumentation along some well-chosen active faults and a bit of luck.

Ring laser observations at Wettzell, Germany, and at Piñon Flat, California, demonstrated consistent measurements of rotational ground motions in the *far field*. So far this success can only be demonstrated with one component of rotation. The high cost of present high-precision ring laser gyros makes widespread deployment of these instruments unlikely. Less expensive (but less sensitive) alternatives are being pursued by several academic groups (Cowsik et al., 2009; Dunn et al., 2009; Jedlička et al., 2009; Schreiber et al., 2009b;

Takamori et al., 2009; Brokesova, 2010; Kozák, 2010; and Velikoseltsev, 2010), and by commercial companies (e.g., Northrop Grumman Litef GmbH, and ATA Sensors).

Schreiber (2011, personal communication) wished to emphasize that their development of a fiber optic gyro (FOG), as reported in Schreiber et al. (2009b), has shown that FOGs are very suitable for measuring ground rotation in the near field of earthquakes, and their recent deployment of a FOG in a building on the campus of the University of Canterbury in Christchurch, New Zealand recorded clear rotational motions in November 14, 2010, from aftershocks of the 3 September 2010 M_W 7 earthquake nearby.

As of late 2010, only Taiwan has a modest program (Lee et al., 2009b) to monitor both translational and rotational ground motions from local and regional earthquakes at several permanent seismic stations, as well as at two arrays in a building and a nearby free-field site. These two arrays are designed to capture a repeat of the 1906 Meishan earthquake (magnitude 7.1) in the *near field* with both translational and rotational instruments in 6-DOF point and array observations (Wu et al., 2009).

Based on the developments described in the *BSSA* Special Issue on rotational seismology and engineering (Lee et al., 2009a), observation, analysis, and interpretation of both rotational and translational ground motions is beginning to play a significant role in seismology and earthquake engineering. An International Working Group on Rotational Seismology (IWGoRS) was organized in 2006 to promote such investigations, evaluate their implications, and share experience, data, software, and results in an open Web-based environment (Todorovska et al., 2008). Anyone can join IWGoRS at http://www.rotational-seismology.org (last accessed 21 January 2011), subscribe to the mailing list, and contribute to the content (publications, data, links, etc.). Finally, the Second IWGoRS Workshop (convened by Johana Brokesova and Heiner Igel) took place 10–13 October 2010 in Prague, Czech Republic (http://www.rotational-seismology.org/events/workshops/2010/2nd-iwgors-workshop, last accessed 21 January 2011) and included contributions from many institutions in several countries.

Acknowledgements

We wish to thank Riccardo DeSalvo, Angela Di Virgilio, Vladimir Graizer, Jan Harms, Brian Kilgore, Jan Kozák, Ulli Schreiber, Chris Stephens, Roman Teisseyre, and Joachim Wassermann for their comments and suggestions, which greatly improve our manuscript.

References

Agnew, D. C. (1986). Strainmeters and tiltmeters. *Rev. Geophys.*, **24**, 579-624.

Aki, K., and Richards, P. G. (2002). *Quantitative Seismology*. 2nd Edition, University Science Books, Sausalito, CA.

Ayden Ö., Akagi, T., and Kawamoto, T. (1993). The squeezing potential of rocks around tunnels: Theory and prediction. *Rock Mech. Rock Eng.*, **2**, 137-163.

Bernauer, M., Fichtner, A., and Igel, H. (2009). Inferring Earth structure from combined measurements of rotational and translational ground motions. *Geophysics*, **74**(6), WCD41-WCD47, doi:10.1190/1.3211110.

Bodin, P., Gomberg, J., Singh, S. K., and Santoyo, M. (1997). Dynamic deformations of shallow sediments in the valley of Mexico, part I: Three dimensional strains and rotations recorded on a seismic array. *Bull. Seism. Soc. Am.*, **87**, 528–539.

Bouchon, M., and Aki, K. (1982). Strain, tilt, and rotation associated with strong ground motion in the vicinity of earthquake faults. *Bull. Seism. Soc. Am.*, **72**, 1717–1738.

Brokesova, J. (2010). Rotaphone - A self-calibrated mechanical seismic sensor for field rotation rate measurements. Second IWGoRS Workshop, October 11-13, Prague, Czech Republic. [Abstract and presentation available at: http://iwgors.pavucina.org/program.php, last accessed 21 January 2011].

Castellani, A., and Guidotti, R. (2010). Free field rotations: Relevance on buildings in near field. Second IWGoRS Workshop, October 11-13, Prague, Czech Republic. [Presentation file available at: http://karel.troja.mff.cuni.cz/~vackar/IWGoRS/Castellani.pdf, last accessed 21 January 2011].

Chi, W. C., Lee, W. H. K., Lin, C. J., and Liu, C. C. (2011). Inversion of ground motion data from a seismometer array using a modification of Jeager's method. [Submitted to the *Bull. Seism. Soc. Am.*, November, 2010.]

Cochard, A., Igel, H., Schuberth, B., Suryanto, W., Velikoseltsev, A., Schreiber, U., Wassermann, J., Scherbaum, F., and Vollmer, D. (2006). Rotational motions in seismology: theory, observation, simulation. In: Teisseyre, R., Takeo, M. and Majewski, E. (ed.), Earthquake Source Asymmetry, Structural Media and Rotation Effects, Springer Verlag, Heidelberg, 391–411.

Cosserat, E., and Cosserat, F. (1909). Théorie des Corps Déformables, Paris: Hermann (available from the Cornell University Library Digital Collections) (in French).

Cowsik, R., Madziwa-Nussinov, T., Wagoner, K., Wiens, D., and Wysession, M. (2009). Performance characteristics of a rotational seismometer for near-field and engineering applications. *Bull. Seism. Soc. Am.*, **99**(2B), 1181–1189.

DeSalvo, R. (2009). Review: accelerometer development for use in gravitational wave-detection interferometers. *Bull. Seism. Soc. Am.*, **99**(2B), 990–997.

Di Virgilio, A. (2010). Installation of the ringlaser G-Pisa inside the Virgo area. Second IWGoRS Workshop, October 11-13, Prague, Czech Republic. [Presentation file available at: http://karel.troja.mff.cuni.cz/~vackar/IWGoRS/Di_Virgilio.pdf, last accessed 21 January 2011]

Droste, Z., and Teisseyre, R. (1976). Rotational and displacemental components of ground motion as deduced from data of the azimuth system of seismograph. *Pub. Inst. Geophys. Polish Acad. Sci.*, **97,** 157–167.

Dunn, R. W., Mahdi, H. H., and Al-Shukri, H. J. (2009). Design of a relatively inexpensive ring laser seismic detector. *Bull. Seism. Soc. Am.*, **99**(2B), 1437–1442.

Evans, J. R., and the International Working Group on Rotational Seismology (2009). Suggested notation conventions for rotational seismology. *Bull. Seism. Soc. Am.*, **99**(2B), 1429–1436.

Evans, J. R., Hutt, C. R., Nigbor, R. L., and de la Torre, T. (2010). Performance of the new R2 Sensor. Second IWGoRS Workshop, October 11-13, Prague, Czech Republic. [Presentation file available at: http://karel.troja.mff.cuni.cz/~vackar/IWGoRS/Evans.pdf, last accessed 21 January 2011].

Farrell, W. E. (1969). A gyroscope seismometer: measurements during the Borrego earthquake. *Bull. Seism. Soc. Am.*, **59**, 1239–1245.

Ferrari, G. (2006). Note on the historical rotation seismographs. In: Teisseyre, R., Takeo, M. and Majewski, E. (ed.), *Earthquake Source Asymmetry, Structural Media and Rotation Effects*, Springer Verlag, Heidelberg, 367–376.

Ferreira, A., and Igel, H. (2009). Rotational motions of seismic surface waves in a laterally heterogeneous Earth. *Bull. Seism. Soc. Am.*, **99**(2B), 1073–1075.

Fichtner, A., and Igel, H. (2009). Sensitivity densities for rotational ground-motion measurements. *Bull. Seism. Soc. Am.*, **99**(2B), 1302–1314.

Galitzin, B. B. (1912). *Lectures on Seismometry.* St. Petersburg: Russian Academy of Sciences, (in Russian).

Gomberg, J., and Agnew, D. (1996). The accuracy of seismic estimates of dynamic strains: an evaluation using strainmeter and seismometer data from Piñon Flat Observatory, California. *Bull. Seism. Soc. Am.*, **86**, 212–220.

Graizer, V. M. (1991). Inertial seismometry methods. *Izv. USSR Acad. Sci., Phys. Solid Earth*, **27**(1), 51–61.

Graizer, V. M. (2005). Effect of tilt on strong motion data processing. *Soil Dyn. Earthq. Eng.*, **25**, 197-204.

Graizer V. (2006). Tilts in strong ground motion. *Bull. Seism. Soc. Am.*, **96**, 2090-2106.

Graizer, V. (2009). Tutorial on measuring rotations using multipendulum systems. *Bull. Seism. Soc. Am.*, **99**(2B), 1064–1072.

Graizer V. (2010). Strong Motion Recordings and Residual Displacements: What Are We Actually Recording in Strong Motion Seismology? *Seism. Res. Lett.*, **81**, 635-639.

Graizer, V., and Kalkan, E. (2010). Strong motion seismology and rotations: History and future directions. Second IWGoRS Workshop, October 11-13, Prague, Czech Republic. [Presentation file available at: http://karel.troja.mff.cuni.cz/~vackar/IWGoRS/Graizer.pdf, last accessed 21 January 2011].

Hinzen, K. G. (2010). Back calculation of earthquake-rotated objects (EROs). Second IWGoRS Workshop, October 11-13, Prague, Czech Republic. [Abstract and presentation available at: http://karel.troja.mff.cuni.cz/~vackar/IWGoRS/Hinzen.pdf, last accessed 21 January 2011].

Huang, B. S. (2003). Ground rotational motions of the 1991 Chi-Chi, Taiwan, earthquake as inferred from dense array observations. *Geophys. Res. Lett.*, **30**(6), 1307–1310.

IEEE-SA Standards Board (1985). IEEE standard specification format guide and test procedure for nongyroscopic inertial angular sensors: jerk, acceleration, velocity, and displacement. *IEEE Std.*, **671-1985**, 69 pp.

Igel, H., Schreiber, U., Flaws, A., Schuberth, B., Velikoseltsev, A., and Cochard, A. (2005). Rotational motions induced by the M8.1 Tokachi-oki earthquake, September 25, 2003. *Geophys. Res. Lett.*, 32: L08309, doi:10.1029/2004GL022336.

Igel, H., Cochard, A., Wassermann, J., Schreiber, U., Velikoseltsev, A., and Pham, N. D. (2007). Broadband observations of rotational ground motions. *Geophys. J. Int.*, **168**, 182–197.

Igel, H. (2010). Observations of long-period rotational ground motions: From ambient noise to Earth's free oscillations. Second IWGoRS Workshop, October 11-13, Prague, Czech Republic. [Presentation file available at: http://karel.troja.mff.cuni.cz/~vackar/IWGoRS/Igel.pdf, last accessed 21 January 2011].

Jedlička, P., Buben, J., and Kozák, J. (2009). Strong-motion fluid rotation seismograph. *Bull. Seism. Soc. Am.*, **99**(2B), 1443–1448.

Kharin, D. A., and Simonov, L. I. (1969). VBPP seismometer for separate registration of translational motion and rotations. *Seismic Instruments*, **5**, 51–66 (in Russian).

Knopoff, L., and Chen, Y. T. (2009). Single-couple component of far-field radiation from dynamical fractures. *Bull. Seism. Soc. Am.*, **99**(2B), 1091–1102.

Kozák, J. T. (2009). Tutorial on earthquake rotational effects: Historical examples. *Bull. Seism. Soc. Am.*, **99**(2B), 998–1010.

Kozák, J. (2010). Pilot sensors for rotation strong motion recording. Second IWGoRS Workshop, October 11-13, Prague, Czech Republic. [Presentation file available at: http://karel.troja.mff.cuni.cz/~vackar/IWGoRS/Kozak.pdf, last accessed 21 January 2011].

Kurrle, D., Igel, H., Ferreira, A. M. G., Wassermann, J., and Schreiber, U. (2010). Can we estimate local Love wave dispersion properties from collocated amplitude measurements of translations and rotations ?. *Geophys. Res. Lett.*, 37, L04307, doi:10.1029/2009GL042215.

Langston, C.A. (2007). Wave gradiometry in two dimensions. *Bull. Seism. Soc. Am.*, **97**, 401–416.

Langston, C. A., Lee, W. H. K., Lin, C. J., and Liu, C. C. (2009). Seismic-wave strain, rotation, and gradiometry for the 4 March 2008 TAIGER explosions. *Bull. Seism. Soc. Am.*, **99**(2B), 1287–1301.

Lantz, B., Schofield, R., O'Reilly, B., Clark, D. E., and DeBra, D. (2009). Review: Requirements for a ground rotation sensor to improve Advanced LIGO. *Bull. Seism. Soc. Am.*, **99**(2B), 980–989.

Lee, V. W., and Trifunac, M. D. (1985). Torsional accelerograms. *Soil Dyn.Earthq. Eng.*, **4**(3), 132–139.

Lee, V. W., and Trifunac, M. D. (1987). Rocking strong earthquake accelerations *Soil Dyn.Earthq. Eng.*, **6**(2), 75–89.

Lee, W. H. K. (Compiler) (2009). A glossary for rotational seismology. *Bull. Seismol. Soc. Am.*, **99**(2B), 1,082–1,090.

Lee, W. H. K., Celebi, M., Igel, H., and Todorovska, M. I. (2009a). Introduction to the Special Issue on Rotational Seismology and Engineering Applications. *Bull. Seism. Soc. Am.*, **99**(2B), 945–957.

Lee, W. H. K., Huang, B. S., Langston, C. A., Lin, C. J., Liu, C. C., Shin, T. C., Teng, T. L., and Wu, C. F. (2009b). Review: Progress in rotational ground-motion observations from explosions and local earthquakes in Taiwan. *Bull. Seism. Soc. Am.*, **99**(2B), 958–967.

Lin, C. J., Huang, H. P., Liu, C. C., and Chiu, H. C. (2010). Application of Rotational Sensors to Correcting Rotation-Induced Effects on Accelerometers. *Bull. Seism. Soc. Am.*, **100,** 585 - 597.

Lin, C. J., Liu, C. C., and Lee, W. H. K. (2009). Recording rotational and translational ground motions of two TAIGER explosions in northeastern Taiwan on 4 March 2008, *Bull. Seism. Soc. Am.*, **99**(2B), 1237–1250.

Liu, C. C., Huang, B. S., Lee, W. H. K., and Lin, C. J. (2009). Observing rotational and translational ground motions at the HGSD station in Taiwan from 2004 to 2008. *Bull. Seism. Soc. Am.*, **99**(2B), 1228–1236.

Mallet, R. (1862). Great Neapolitan Earthquake of 1857, I and II. Chapman and Hall, London.

McLeod, D. P., Stedman, G. E., Webb, T. H., and Schreiber, U. (1998). Comparison of standard and ring laser rotational seismograms. *Bull. Seism. Soc. Am.*, **88**, 1495–1503.

Nigbor, R. L. (1994). Six-degree-of-freedom ground motion measurement. *Bull. Seism. Soc. Am.*, **84**, 1665–1669.

Nigbor, R. L., Evans, J. R., and Hutt, C. R. (2009). Laboratory and field testing of commercial rotational seismometers. *Bull. Seism. Soc. Am.*, **99**(2B), 1215–1227.

Oldham, R. D. (1899). Report on the Great Earthquake of 12th June 1897, *Memoir of the Geological Survey of India*, **29**.

Oliveira, C. S., and Bolt, B. A. (1989). Rotational components of surface strong ground motion. *Earthq. Eng. Struct. Dyn.*, **18**, 517–526.

Pham, D. N., Igel, H., Wassermann, J., Cochard, A., and Schreiber, U. (2009). The effects of tilt on interferometric rotation sensors. *Bull. Seism. Soc. Am.*, **99**(2B), 1352–1365.

Pujol, J. (2009). Tutorial on rotations in the theories of finite deformation and micropolar (Cosserat) elasticity. *Bull. Seism. Soc. Am.*, **99**(2B), 1011–1027.

Reid, H. F. (1910). The Mechanics of the Earthquake. *The California Earthquake of April 18, 1906, Report of the State Earthquake Investigation Commission, Volume 2.* Carnegie Institution of Washington, 43–47.

Richter, C. F. (1958). Elementary Seismology. W. H. Freeman & Co, San Francisco, CA.

Schreiber, K. U., Igel, H., Cochard, A., Velikoseltsev, A., Flaws, A., Schuberth, B., Drewitz, W., and Müller, F. (2005). The GEOsensor project: rotations — a new observable for seismology. In: Flury, Rummel, J., R., Reigber, C., and Rothacher, M. (ed.), *Observation of the Earth System from Space*. Heidelberg: Springer Verlag, 1–19.

Schreiber, K. U., Hautmann, J. N., Velikoseltsev, A., Wassermann, J., Igel, H., Otero, J., Vernon, F., and Wells, J.-P. R. (2009a). Ring laser measurements of ground rotations for seismology. *Bull. Seism. Soc. Am.*, **99**(2B), 1190–1198.

Schreiber, K. U., Velikoseltsev, A., Carr, A. J., and Franco-Anaya, R. (2009b). The application of fiber optic gyroscopes for the measurement of rotations in structural engineering. *Bull. Seism. Soc. Am.*, **99**(2B), 1207–1214.

Schreiber, K. U. (2010). Progress in ring laser technology. Second IWGoRS Workshop, October 11-13, Prague, Czech Republic. [Presentation file available at: http://karel.troja.mff.cuni.cz/~vackar/IWGoRS/Schreiber.pdf, last accessed 21 January 2011].

Schreiber, K. U., Velikoseltsev, A., Bosse, H., and Krause, M. (2011). The comparison of µFORS and R-1 rotation sensors, unpublished report.

Segall, P. (2010). *Earthquake and Volcano Deformation*. Princeton Univ. Press, Princeton and Oxford.

Smith, D. (2010). ATA's nanoradian-class rotational sensors. Second IWGoRS Workshop, October 11-13, Prague, Czech Republic. [Poster file available at: http://karel.troja.mff.cuni.cz/~vackar/IWGoRS/Smith_poster.pdf, last accessed 21 January 2011].

Spudich, P., Steck, L. K., Hellweg, M., Fletcher, J. B., and Baker, L. M. (1995). Transient stresses at Parkfield, California, produced by the M 7.4 Landers earthquake of June 28, 1992: Observations from the UPSAR dense seismograph array. *J. Geophys. Res.*, **100**(B1), 675–690.

Spudich, P., and Fletcher, J. B. (2008). Observation and prediction of dynamic ground strains, tilts, and torsions caused by the Mw 6.0 2004 Parkfield, California, earthquake and aftershocks, derived from UPSAR Array observations. *Bull. Seism. Soc. Am.*, **98**, 1898–1914.

Spudich, P., and Fletcher J. B. (2009). Software for inference of dynamic ground strains and rotations and their errors from short baseline array observations of ground motions. *Bull. Seism. Soc. Am.*, **99**(2B), 1480–1482.

Stedman, G. E. (1997). Ring laser tests of fundamental physics and geophysics. *Rept. Progress Phys*., **60**, 615–688.

Stupazzini, M., De La Puente, J., Smerzini, C., Kaser, M., Igel, H., and Castellani, A. (2009). Study of rotational ground motion in the near field region. *Bull. Seism. Soc. Am.*, **99**(2B), 1271–1286.

Suryanto, W., Igel, H., Wassermann, J., Cochard, A., Schuberth, B., Vollmer, D., Scherbaum, F., Schreiber, U., and Velikoseltsev, A. (2006). First comparison of array-derived rotational ground motions with direct ring laser measurements. *Bull. Seism. Soc. Am.*, **96**, 2059–2071.

Takamori, A., Araya, A., Otake, Y., Ishidoshiro, K., and Ando, M. (2009). Research and development status of a new rotational seismometer based on the flux pinning effect of a superconductor. *Bull. Seism. Soc. Am.*, **99**(2B), 1174–1180.

Takeo, M. (1998). Ground rotational motions recorded in near-source region. *Geophys. Res. Lett.*, **25**(6), 789–792.

Takeo, M. (2009). Rotational motions observed during an earthquake swarm in April, 1998, at offshore Ito, Japan. *Bull. Seism. Soc. Am.*, **99**(2B), 1457–1467.

Takeo, M., and Ito, H. M. (1997). What can be learned from rotational motions excited by earthquakes? *Geophys. J. Int.*, **129**, 319–329.

Teisseyre, R., Takeo, M., and Majewski, E. (editors) (2006). *Earthquake Source Asymmetry, Structural Media and Rotation Effects*. Springer-Verlag, Berlin-Heidelberg.

Teisseyre, R., Nagahama, H., and Majewski, E. (editors) (2008). *Physics of Asymmetric Continua: Extreme and Fracture Processes: Earthquake Rotation and Soliton Waves.* Springer-Verlag, Berlin-Heidelberg.

Teisseyre, R. (2010). Why rotation seismology: Confrontation between classic and asymmetric theories. Second IWGoRS Workshop, October 11-13, Prague, Czech Republic. [Presentation file available at: http://karel.troja.mff.cuni.cz/~vackar/IWGoRS/R_Teisseyre.pdf, last accessed 21 January 2011].

Todorovska, M. I., and Trifunac, M. D. (1990). Note on excitation of long structures by ground waves. *Am. Soc. Civil Eng., Eng. Mech. Div.*, **116**(4): 952–964.

Todorovska, M. I., Igel, H., Trifunac, M. D., and Lee, W. H. K. (2008). Rotational earthquake motions – International working group and its activities. Proceedings of the 14th World Conference on Earthquake Engineering, October 12-17, Beijing, China, Paper ID: S03-02-0031.

Trifunac, M. D. (1979). A note on surface strains associated with incident body waves. *Bull. European Assoc. Earthq. Eng.*, **5**, 85–95.

Trifunac, M. D. (1982). A note on rotational components of earthquake motions on ground surface for incident body waves. *Soil Dyn. Earthq. Eng.*, **1**, 11–19.

Trifunac, M. D. (2006). Effects of torsional and rocking excitations on the response of structures. In: Teisseyre, R., Takeo, M. and Majewski, E. (ed.), *Earthquake Source Asymmetry, Structural Media and Rotation Effects*, p. 569–582, Springer Verlag, Heidelberg.

Trifunac, M. D. (2009). Earthquake engineering, nonlinear problems in. In: Meyers, R.A. (ed.), *Encyclopedia of Complexity and Systems Science*, p. 2421–2437, Springer, New York.

Trnkoczy, A., P. Bormann, W. Hanka, L. G. Holcomb, and R. L. Nigbor (2002). Site Selection, Preparation and Installation of Seismic Stations. In: *New Manual of Seismological Observatory Practice (NMSOP)*, edited by Bormann, P., Chapter 7, GeoForschungsZentrum, Potsdam, Germany.

Twiss, R. J. (2009). An asymmetric micropolar moment tensor derived from a discrete-block model for a rotating granular substructure. *Bull. Seism. Soc. Am.*, **99**(2B), 1103–1131.

Twiss, R., Souter, B., and Unruh, J. (1993). The effect of block rotations on the global seismic moment tensor and patterns of seismic P and T axes. *J. Geophys. Res.*, **98**, 645–674.

Velikoseltsev, A. (2010). Fiber optic gyroscope as a tool for detection of seismic rotations. Second IWGoRS Workshop, October 11-13, Prague, Czech Republic. [Presentation file available at: http://karel.troja.mff.cuni.cz/~vackar/IWGoRS/Velikoseltsev.pdf, last accessed 21 January 2011].

Wang, H., Igel, H., Gallovic, F., and Cochard, A. (2009). Source and basin effects of rotations: Comparison with translations. *Bull. Seism. Soc. Am.*, **99**(2B), 1162–1173.

Wassermann, J., Lehndorfer, S., Igel, H., and Schreiber, U. (2009). Performance test of a commercial rotational motions sensor. *Bull. Seism. Soc. Am.*, **99**(2B), 1449–1456.

Wu, C. F., Lee, W. H. K., and Huang, H. C. (2009). Array deployment to observe rotational and translational ground motions along the Meishan fault, Taiwan: A progress report. *Bull. Seism. Soc. Am.*, **99**(2B), 1468–1474.